

An HSP90 inhibitor overcomes *EGFR* amplification-induced resistance to third-generation EGFR-TKIs

HSP90 inhibitors overcome TKI-resistance

Sho WATANABE^{1,2,3}, Yasushi GOTO², Hiroyuki YASUDA⁴, Takashi KOHNO⁵, Noriko MOTOI⁶, Yuichiro OHE², Hiroyoshi NISHIKAWA¹, Susumu S. KOBAYASHI^{7, 8}, Kazuyoshi KUWANO³, and Yosuke TOGASHI¹

¹Division of Cancer Immunology, ⁵Genome Biology, and ⁷Translational Genomics, Research Institute / Exploratory Oncology Research & Clinical Trial Center (EPOC), National Cancer Center, Tokyo/Chiba, Japan.

²Department of Thoracic Oncology, and ⁶Pathology and Clinical Laboratories, National Cancer Center Hospital, Tokyo, Japan.

³Department of Respiratory Medicine, Jikei University of Medicine, Tokyo, Japan.

⁴Division of Pulmonary Medicine, Department of Medicine, Keio University, School of Medicine, Tokyo, Japan.

⁸Department of Medicine, Beth Israel Deaconess Medical Center, Boston, MA, USA

Corresponding authors:

Yasushi Goto, MD. PhD,

Department of Thoracic Oncology, National Cancer Center Hospital, 1-1, Tsukiji 5,

Chuo-ku, Tokyo 104-0045, Japan.

Phone: +81-3-3542-2511, FAX: +81-3-3542-3815

E-mail: ygoto@ncc.go.jp

Yosuke Togashi, MD. PhD,

Division of Cancer Immunology, Research Institute / Exploratory Oncology Research &
Clinical Trial Center (EPOC), National Cancer Center, Tokyo/Chiba, Japan.

Phone: +81-4-7130-1111, Fax: +81-4-7130-0022.

E-mail: ytogashi1584@gmail.com

Abstract:

Background: Patients with non-small cell lung cancer (NSCLC) harboring activating *EGFR* mutations are sensitive to epidermal growth factor receptor-tyrosine kinase inhibitors (EGFR-TKIs) but inevitably develop resistance to the inhibitors mostly through acquisition of the secondary *T790M* mutation. Though third-generation EGFR-TKIs overcome this resistance by selectively inhibiting EGFR with EGFR-TKI-sensitizing and *T790M* mutations, acquired resistance to third-generation EGFR-TKIs invariably develops.

Methods: Next-generation sequencing (NGS) and fluorescence *in situ* hybridization (FISH) analysis were performed in an *EGFR T790M*-mutated NSCLC patient who progressed after a third-generation EGFR-TKI, TAS-121. *EGFR*-mutated cell lines were subjected to a cell proliferation assay and western blotting analysis with EGFR-TKIs and a heat shock protein 90 (HSP90) inhibitor.

Results: NGS and FISH analysis revealed *EGFR* amplification in the resistant cancer cells. While *EGFR L858R/T90M*-mutated cell line was sensitive to osimertinib or TAS-121 *in vitro*, *EGFR*-overexpressing cell lines displayed resistance to these EGFR-TKIs. Western blot analysis showed that EGFR phosphorylation in the *EGFR*-overexpressing cell lines was not suppressed by third-generation EGFR-TKIs. In contrast, an HSP90 inhibitor reduced total and phosphorylated EGFR and inhibited the proliferation of resistant cell lines.

Conclusions: *EGFR* amplification confer the resistance to third-generation EGFR-TKIs, which can be overcome by HSP90 inhibition. The results provide a preclinical rationale for the use of HSP90 inhibitors to overcome the *EGFR* amplification-mediated resistance.

Key points:

Significant findings of the study:

EGFR-amplification conferred the resistance to a third-generation *EGFR*-TKI in an *EGFR T790M*-mutated NSCLC patient. Inhibiting HSP90, a chaperon for *EGFR*, can overcome the *EGFR* amplification-mediated resistance.

What this study adds:

The efficacy of HSP90 inhibitor *in vitro* and *in vivo* provides a preclinical rationale for the use of HSP90 inhibitors to overcome the *EGFR* amplification-mediated resistance to third-generation *EGFR*-TKIs.

Keywords:

Acquired resistance, epidermal growth factor receptor, epidermal growth factor receptor amplification, epidermal growth factor receptor-tyrosine kinase inhibitor, and heat shock protein 90

Introduction

Epidermal growth factor receptor (*EGFR*) mutations are commonly found in non-small cell lung cancer (NSCLC), with a prevalence of 10-20 % in Caucasian patients and 30-40% in Asian patients with advanced NSCLC^{1, 2}. Upon mutation of the tyrosine kinase domains of *EGFR*, *EGFR* undergoes conformational changes, and its equilibrium is shifted towards a ligand-independent activated state³, which results in cell proliferation or survival⁴. Activating *EGFR* mutations (in-frame deletions in exon 19 and a point mutation in exon 21) trigger tumorigenesis and are a major determinant of susceptibility to *EGFR* tyrosine kinase inhibitors (*EGFR*-TKIs)⁵. Numerous clinical trials have shown the superior efficacy of first-generation *EGFR*-TKIs (gefitinib and erlotinib) or second-generation *EGFR*-TKIs (afatinib) compared with chemotherapy⁶⁻¹¹ and have established these agents as the standard of care for advanced *EGFR*-mutated NSCLC.

Despite their marked response to *EGFR*-TKIs, *EGFR*-mutated NSCLCs inevitably develop resistance to these inhibitors after approximately 8-13 months of treatment⁵. Among the resistance mechanisms, the *EGFR* T790M mutation is predominant, occurring in approximately half of *EGFR*-mutated NSCLC cases^{5, 12, 13}. However, this limitation has been overcome by the introduction of third-generation *EGFR*-TKIs, such as osimertinib. These compounds covalently bind to the C797 residue

within the mutant EGFR kinase domain, irreversibly binding to the ATP-binding site while sparing wild-type EGFR¹⁴⁻¹⁶. These characteristics of third-generation EGFR-TKIs have led to their significant efficacy and decreased toxicity in clinical trials^{17, 18}, and osimertinib has been approved for the treatment of *EGFR*-positive NSCLC patients¹⁹.

Similar to patients treated with earlier-generation EGFR-TKIs, those receiving third-generation EGFR-TKIs invariably develop drug resistance. Identification of the resistance mechanisms is crucial for improving outcomes in patients with *EGFR*-mutated NSCLC. Heterogeneous mechanisms underlying resistance to third-generation EGFR-TKIs have been reported; these include the tertiary *EGFR* C797S mutation; amplification of *MET* or *HER2*; mutations in *PIK3CA*, *ALK*, or *BRAF*; and *RET* fusions²⁰. However, the resistance mechanisms are not fully understood and are unknown in 30-50% of cases²¹, necessitating their further investigation.

Heat shock proteins (HSPs) assist in the folding of nascent polypeptides into a functional conformation, thus facilitating protein stability and turnover, which are necessary for the intracellular localization and function of proteins²². The HSP90 chaperone machinery, a key regulator of proteostasis, impairs apoptotic signaling in cancer cells²³. Since EGFR is a client protein for the HSP90 chaperone, a strategy of targeting HSP90 has been evaluated in *EGFR*-mutated NSCLC²⁴. While clinical trials

have shown the activity of HSP90 inhibitors in NSCLC patients harboring *EGFR* mutations^{25, 26}, whether inhibition of HSP90 can overcome acquired resistance to third-generation EGFR-TKIs remains to be determined.

Here, we report a resistance mechanism of *EGFR* amplification in a patient with *EGFR* T790M-mutated NSCLC who developed acquired resistance to a third-generation EGFR-TKI, TAS-121¹⁶. Then, we investigated the role of *EGFR* amplification in this resistance *in vitro*. Furthermore, we evaluated the sensitivity of this tumor to an HSP90 inhibitor (TAS-116)²⁷ to evaluate the therapeutic possibility of a potent HSP90 inhibitor.

Methods

Patient and samples

Tumor samples were obtained by biopsy and autopsy from a patient with metastatic lung adenocarcinoma harboring an *EGFR* L858R mutation and were analyzed by next-generation sequencing (NGS) and/or fluorescence *in situ* hybridization (FISH).

NGS of clinical samples

NGS (NCC OncoPanel v3, Agilent Technologies, Santa Clara, CA) was performed using formalin-fixed, paraffin-embedded (FFPE) samples obtained from a progressing liver

lesion during TAS-121 therapy as previously described^{28, 29}. Sequenced genes are summarized in **Supplementary Table S1**.

FISH analysis

We conducted FISH analysis for *EGFR* with a Vysis EGFR Dual Color Probe-Hyb Set (Abbott Laboratories, Abbott Park, IL) using FFPE samples from pre-TAS-121-treatment liver lesions, post-TAS-121-treatment liver lesions, and autopsied lung and liver lesions. *EGFR* amplification was indicated if the EGFR/CEP signal ratio was >2.0 ³⁰.

Cell lines and reagents

The HCC827 and H1975 cell lines (human NSCLC cell lines) were obtained from the American Type Culture Collection (ATCC; Manassas, VA), and the PC-9 cell line (a human NSCLC cell line) was obtained from the European Collection of Authenticated Cell Cultures (ECACC; Salisbury, UK). The PC9-COR cell line was established from the PC-9 cell line as previously reported³¹. All cell lines were authenticated using the short tandem repeat method and were maintained in RPMI medium (FUJIFILM Wako Pure Chemical Corporation, Osaka, Japan) supplemented with 10% fetal bovine serum (FBS; Cytiva, Marlborough, MA). The *EGFR* status of the cell lines is summarized in

Supplementary Table S2. All cell lines were used after they were confirmed to be negative for *Mycoplasma* contamination with a PCR Mycoplasma Detection Kit (TaKaRa Bio, Shiga, Japan) according to the manufacturer's instructions. Erlotinib and osimertinib were obtained from Cayman Chemical Company (Ann Arbor, MI). TAS-121 and TAS-116 were kindly provided by Taiho Pharmaceutical Co., Ltd. (Tokyo, Japan).

Cell proliferation assay

Cells were plated in 96-well plates at a density of 2×10^3 cells/well and incubated for 24 hours. Cell proliferation was evaluated with a WST-1 assay (TaKaRa Bio) after 72 hours of treatment. The absorption of WST-1 was measured at a wavelength of 450 nm with a reference wavelength of 690 nm in a microplate reader. Cell viability was calculated as the ratio of the absorbance value of the treated cells to that of the control cells and expressed as a percentage. Experiments were performed independently in triplicate.

Establishment of the *EGFR* L858R/T790M-overexpressing H1975 cell line

H1975 cells with overexpression of *EGFR* L858R/T790M (H1975-LR/TM) were generated by retroviral transduction. In brief, packaging cells were transfected with pBABE-puro-*EGFR* L858R/T790M or a control pBABE-puro-mock vector (Addgene,

Watertown, MA) and a VSV-G vector (TaKaRa Bio) using Lipofectamine 3000 (Thermo Fisher Scientific, Waltham, MA). Viral supernatant was collected 2 days after transfection, and viral particles were transduced into H1975 cells.

Western blotting

Subconfluent cells were washed with PBS and harvested with M-PER (Thermo Fisher Scientific, Waltham, MA). Whole-cell lysates were separated by SDS-PAGE and transferred to a polyvinylidene fluoride membrane. After blocking, the membrane was probed with a primary antibody. After two rinses with TBS-T buffer, the membrane was incubated with a horseradish peroxidase-conjugated secondary antibody and washed. Immunoreactions were visualized using an ECL detection system and a LAS-4000 (GE Healthcare, Chicago, IL). Antibodies are summarized in **Supplementary Table S3**. Experiments were performed independently in at least triplicate.

Apoptosis

Apoptosis was assessed using flowcytometry with FITC-annexin V and 7-AAD (Thermo Fisher Scientific). The staining reagents were diluted in accordance with the manufacturer's instructions. The stained cells were analyzed with the LSR Fortessa (BD

Biosciences) and FlowJo software (BD Biosciences).

Xenograft studies

Female BALB/c nu/nu nude mice (6–8 weeks old) were purchased from CLEA Japan (Tokyo, Japan). H1975 cells, H1975-LR/TM, and PC9-COR cells (1×10^6) in 100 μ L of RPMI with 100 μ L of Matrigel were injected subcutaneously, and the tumor volume was assessed twice a week using the formula “length \times width² \times 0.5.” The mice were grouped when the tumor volume reached approximately 200–500 mm³. TAS-121 (12.5 mg/kg/day) and the vehicle were orally administered daily, and TAS-116 (14 mg/kg/day) was orally administered five times a week thereafter. All the mice were maintained under specific pathogen-free conditions in the animal facility of the Institute of Biophysics. The mouse experiments were approved by the Animal Committee for Animal Experimentation of the National Cancer Center. All the experiments met the guidelines of the US Public Health Service Policy on Humane Care and Use of Laboratory Animals.

Statistics analyses

Continuous variables were analyzed using a t-test. The relationship between the tumor volume curves were compared using a two-way ANOVA. Statistical analyses were two-

tailed and performed with the Prism version 7 software (GraphPad Software, Inc., La Jolla, CA, USA). A *p*-value of less than 0.05 was considered statistically significant.

Results

Clinical course

A 68-year-old woman with metastatic lung adenocarcinoma (cT4N2M1b, stage IV) harboring the *EGFR* L858R mutation received gefitinib treatment and achieved a partial response (PR) (**Figure 1**). Eleven months later, she experienced progressive disease (PD) and subsequently received 4 cycles of chemotherapy with cisplatin and pemetrexed followed by pemetrexed maintenance therapy. Computed tomography (CT) after 6 months of chemotherapy showed disease progression with liver metastases. Tumor progression was also noted after completion of one cycle of docetaxel, and rebiopsy of a progressing liver lesion was performed. Tumor genotyping with the peptide nucleic acid-locked nucleic acid (PNA-LNA) PCR clamp method revealed a secondary mutation of *EGFR* T790M in addition to the primary *EGFR* L858R mutation. She was enrolled in a phase I trial of TAS-121 (12 mg/day)³². Despite initial PR, PD was confirmed by CT after 3 months, indicating progression of liver metastases whereas lung lesions were stable. Then, rebiopsy of the progressive liver lesion was performed. She discontinued TAS-121

and received best supportive care. She died 4 months after initiation of TAS-121 treatment, and an autopsy was performed.

***EGFR* was amplified in the patient with acquired resistance to TAS-121**

NGS of the progressive liver lesion post TAS-121 treatment revealed *EGFR* amplification (log₂ ratio = 2.2). Whereas both the wild-type and T790M-mutated *EGFR* alleles were amplified, the mutated allele was dominant (**Figure 2A**). In contrast, we could not find any typical genetic alterations that can cause resistance to third-generation EGFR-TKIs (i.e., *MET* amplification or *EGFR* C797S mutation; **Supplementary Tables S1 and S4**). According to the definition of *EGFR* amplification, which is an EGFR/CEP signal ratio > 2.0 by FISH analysis³⁰, no *EGFR* amplification was identified in the pre-TAS-121-treatment liver lesion (EGFR/CEP signal ratio, 1.7) but was detected in both the rebiopsied post-TAS-121-treatment and autopsied liver lesions (2.1 and 3.0, respectively; **Figure 2B**). *EGFR* amplification was not observed in the autopsied lung lesions (1.0), which did not progress during TAS-121 treatment. These findings suggest that the patient acquired resistance to TAS-121 owing to the *EGFR* amplification mainly of the mutated allele.

Third-generation EGFR-TKIs, including TAS-121, effectively inhibit the proliferation of *EGFR*-mutated NSCLC cells

To verify the efficacy of EGFR-TKIs in *EGFR*-mutated cell lines, we evaluated sensitivity to the inhibitors *in vitro*. As expected, the HCC827 and PC-9 cell lines carrying the activating *EGFR* exon 19 deletion mutation were sensitive to erlotinib (a first-generation EGFR-TKI) and to osimertinib and TAS-121 (third-generation EGFR-TKIs) (**Figure 3A**). The proliferation of H1975 cells harboring the T790M resistance and L858R sensitizing mutations was inhibited by osimertinib and TAS-121 but not by erlotinib (**Figure 3A**). Consistent with this result, western blot analysis showed that osimertinib and TAS-121 reduced phosphorylation of EGFR and the downstream AKT and ERK in the H1975 cell line in a dose-dependent manner as well as in the PC-9 cell line, whereas erlotinib did not decrease phosphorylation in the H1975 cell line (**Figure 3B and C**). Apoptosis was significantly induced by all EGFR-TKIs in the PC-9 cell line (**Figure 3D**). In contrast, erlotinib did not induce apoptosis, whereas TAS-121 as well as osimertinib significantly induced apoptosis in the H1975 cell line (**Figure 3E**). These findings confirm that TAS-121, a third-generation EGFR-TKI, overcomes the *EGFR* T790M-driven resistance to erlotinib by a mechanism similar to that of osimertinib¹⁶.

***EGFR* amplification mediates resistance to third-generation EGFR-TKIs**

The results of NGS data analysis and FISH analysis in our patient suggested that amplification of *EGFR*, especially the T790M mutant, occurred upon resistance to TAS-121. Thus, we used retroviral transduction to generate an H1975 cell line with overexpression of L858R/T790M-mutated *EGFR* (H1975-LR/TM), and we evaluated inhibitor sensitivities *in vitro*. **Figure 4A** shows that H1975-LR/TM cells contained higher levels of phosphorylated and total EGFR than control cells. In the cell proliferation assay, the H1975-LR/TM cell line was resistant to both TAS-121 and osimertinib (**Figure 4B**). These results were supported by those of western blot analysis; that is, TAS-121 and osimertinib did not inhibit phosphorylation of EGFR and the downstream AKT and ERK in the H1975-LR/TM cell line (**Figure 4C**). Consistently, apoptosis was not induced by TAS-121 and osimertinib in this cell line (**Figure 4D**). These findings suggest that amplification of the mutated *EGFR* gene mediated the resistance to TAS-121 in this patient.

The image generated by Interactive Genome Viewer showing the possible coemergence of the wild-type *EGFR* allele prompted us to evaluate the effects of EGFR-TKIs on the PC9-COR cell line with amplification of wild-type *EGFR*, which was previously established using rociletinib as a clone resistant to erlotinib and third-

generation EGFR-TKIs³¹ (**Figure 2A**). We confirmed the expression of not mutated but wild-type EGFR in PC9-COR cells (**Figure 5A**). Accordingly, the PC9-COR cell line displayed resistance to TAS-121 as well as to erlotinib and osimertinib (**Figure 5B**), and western blot analysis showed that no EGFR-TKI reduced phosphorylation of EGFR and the downstream AKT and ERK (**Figure 5C**). Apoptosis was not induced by these EGFR-TKIs in this cell line (**Figure 5D**). These findings are consistent with those of a previous study showing that amplification of wild-type *EGFR* also mediates resistance to third-generation EGFR-TKIs³¹. Taken together, these results indicate that amplification of both mutated and wild-type *EGFR* can mediate resistance to third-generation EGFR-TKIs.

An HSP90 inhibitor, TAS-116, overcomes *EGFR* amplification-mediated acquired resistance to third-generation EGFR-TKIs

To explore the possibility that HSP90 inhibition can overcome *EGFR* amplification-mediated resistance, we analyzed the sensitivities of PC-9, H1975, H1975-LR/TM and PC9-COR cell lines to the HSP90 inhibitor TAS-116 *in vitro*. Parent cell lines (PC-9 and H1975) were sensitive to TAS-116 (**Supplementary Figure S1**). Additionally, the viability of both H1975-LR/TM and PC9-COR cells was compromised by treatment with the HSP90 inhibitor (**Figure 4B and Figure 5B**). Importantly, TAS-116 was highly active

against these cell lines at therapeutic concentrations of 1-3 μM ^{33, 34}. In contrast, the combination efficacy of TAS-121 and TAS-116 was not observed in both the H1975 and H1975-LR/TM cell lines (**Supplementary Figure S1**). Consistent with this finding, TAS-116 greatly reduced the levels of both total and phosphorylated EGFR and the downstream AKT and ERK in these cell lines in a concentration-dependent manner (**Figure 4C and Figure 5C**). Apoptosis was also significantly induced by TAS-116 (**Figures 4D and 5D**). Furthermore, the *in vivo* effects of TAS-116 against both H1975-LR/TM and PC9-COR tumors that were resistant to TAS-121 were also observed (**Figure 6A-C**). These results provide a preclinical rationale for the use of HSP90 inhibitors to overcome the acquired resistance to third-generation EGFR-TKIs induced by *EGFR* amplification.

Discussion

In this study, we identified mutated *EGFR* amplification as a resistance mechanism in a patient with *EGFR* T790M-positive NSCLC who experienced PD on a third-generation EGFR-TKI, TAS-121. *In vitro*, amplification of not only wild-type but also mutated *EGFR* induced resistance. This is the first case of mutated *EGFR* amplification-mediated resistance in a patient treated with TAS-121, although this mechanism has been reported

in patients treated with other third-generation EGFR-TKIs^{35, 36}. In addition, TAS-116 overcame this resistance *in vitro* and *in vivo*, indicating that HSP90 inhibition is a therapeutic strategy for patients with *EGFR* amplification-mediated resistance to third-generation EGFR-TKIs.

Acquired resistance has been a challenge in EGFR-TKI therapy. Initial characterization of resistance to earlier-generation EGFR-TKIs identified *EGFR* T790M mutation as a predominant resistance mechanism and led to the development of third-generation EGFR-TKIs⁵. However, the efficacy of third-generation EGFR-TKIs has been limited by the occurrence of secondary resistance²⁰. Numerous studies have shown the heterogeneity of mechanisms underlying resistance to third-generation EGFR-TKIs. In addition to the tertiary resistance *EGFR* C797S mutation, somatic copy number alterations account for a substantial portion of resistance^{21, 37}. From our NGS data, we identified *EGFR* amplification as a resistance mechanism, but no other alterations, including *MET* amplification and *EGFR* C797S mutation, were identified as resistance mechanisms. Consistent with our findings, a prior study reported that amplification of mutated *EGFR* emerged in 39% of plasma samples from patients with acquired resistance to earlier-generation EGFR-TKIs and 9% of those from patients with resistance to a third-generation EGFR-TKI³⁸. Amplification of the T790M allele was also confirmed in 23%

of biopsy samples from patients with T790M-positive NSCLC at development of resistance to a third-generation EGFR-TKI³⁵. Understandably, amplification of wild-type *EGFR* can confer resistance to third-generation EGFR-TKIs because third-generation EGFR-TKIs selectively inhibit mutated EGFR and allow wild-type EGFR to escape inhibition⁵. Indeed, amplification of wild-type *EGFR* was reported to decrease the sensitivity of *EGFR*-mutated cancer cells to third-generation EGFR-TKIs *in vitro*^{31, 38, 39} and to cause resistance to osimertinib in a patient with T790M-positive NSCLC⁴⁰. Conversely, in the clinical setting, accumulating evidence, including our case, indicates that amplification of mutated *EGFR* drives resistance to these inhibitors despite the potent inhibition of mutant EGFR by third-generation EGFR-TKIs^{35, 38, 41}. These conflicting results highlight the need for an improved understanding of *EGFR* amplification-mediated resistance. Here, we found that the overexpression of mutated *EGFR* outpaced the inhibitory activity of third-generation EGFR-TKIs, providing additional insight into the interplay between *EGFR* amplification and the response to EGFR-TKIs. In addition, the increasing use of circulating tumor DNA in blood to clarify resistance mechanisms may favor the reporting of amplification of mutated *EGFR*, because the inevitable contamination by nonmalignant cells hinders clinicians from accurately analyzing the copy numbers of wild-type genes³¹. Thus, the association between the copy numbers of

mutated *EGFR* and EGFR inhibition needs further investigation to determine minimum amplification threshold for induction of resistance, and analyzing not only *EGFR* mutations but also *EGFR* copy numbers can facilitate access to optimal therapies in clinical settings.

In our patient, CT on the failure of TAS-121 therapy showed mixed response to the agent; among the multiple lesions in the lung and liver, only liver metastasis progressed, and the lung lesions did not change in size. In the FISH analysis, *EGFR* amplification was found in the resistant liver lesions but not in the lung lesions, which suggests that heterogeneous cancer cells emerged with resistant *EGFR*-amplified cancer cells in the liver metastases. Indeed, the results of an ongoing clinical trial raised the possibility that a focal copy number gain occurred subclonally upon the development of osimertinib resistance and was spatially and temporally separated from common resistance mechanisms, such as C797S mutation⁴². Thus, the *EGFR* amplification in resistant liver lesions in our patient could reflect the evolutionary process of subclones selected by the potent EGFR-inhibitory effects of TAS-121 and demanded to selectively target *EGFR* amplification to overcome the resistance.

HSP90 inhibitors have exhibited potent antitumor activities in various preclinical models by destabilizing HSP90 client proteins⁴³. Importantly, mutated EGFR proteins are

particularly reliant on the chaperone activity of HSP90 for their conformational stability and function⁴⁴, which led the H1975-LR/TM cell line harboring the mutated *EGFR* amplification to have higher sensitivity than the PC9-COR cell line with wild-type *EGFR* amplification to TAS-116 in our present study. In clinical trials, luminespib, a member of another class of HSP90 inhibitors, exhibited activity against *EGFR*-mutated NSCLC^{25, 26}. Consistent with this finding, our present study shows that TAS-116 exhibited efficacies against parent *EGFR*-mutated cell lines sensitive to EGFR-TKIs. In addition, HSP90 inhibition alone reportedly overcame the *MET* amplification- or HGF-induced resistance to EGFR-TKIs *in vitro*^{45, 46}. Luminespib combined with osimertinib exhibited a marked efficacy for intrinsic resistance to osimertinib by decreasing the phosphorylation of EGFR and MET and downregulating their downstream pathways⁴⁷. Our present study also showed that AKT and ERK, the downstream signals in the EGFR pathway, were degraded by HSP90 inhibition using TAS-116, which supports the use of HSP90 inhibitors to overcome the resistance to EGFR-TKIs.

Our patient received third-generation EGFR-TKI after acquired resistance to gefitinib because at that time, no first-line osimertinib therapy had been established. Consequently, we identified EGFR amplification as a resistance mechanism to fourth-line third-generation EGFR-TKI. However, first-line osimertinib therapy is a standard of care

in the current clinical setting, and whether *EGFR* amplification can confer resistance to third-generation EGFR-TKIs regardless of the treatment lines with EGFR-TKIs remains uncertain. In a previous study, *EGFR* amplification induced resistance to first-line third-generation EGFR-TKIs²¹. An osimertinib-resistant PC9-COR cell line represented the resistance to first-line third-generation EGFR-TKIs³¹, which was overcome by TAS-116 in our study. Thus, HSP90 inhibitors can also overcome *EGFR* amplification-mediated resistance to first-line third-generation EGFR-TKIs.

HSP90 inhibitors have shown limited efficacy as single agents⁴³. Undesirable off-target and/or HSP90-related adverse events could account for this discrepancy via the need to limit the drug concentrations to levels insufficient to efficiently suppress intratumoral HSP90 activity²⁴. The most common adverse event in patients receiving HSP90 inhibitors was visual disorders due to sustained HSP90 inhibition in the retina⁴⁸. TAS-116 possesses a distinct advantage over other HSP90 inhibitors, as its distribution in retinal tissue is lower than that in plasma, and it is rapidly eliminated from the retina²⁷. Indeed, eye disorders were not clinically significant in trials for patients with advanced solid tumors^{33, 34}. Therefore, further studies should focus on TAS-116 as a promising therapeutic option for *EGFR*-mutated lung cancer. Especially, patient-derived experiments (xenograft model and patient-derived cell line or organoid) would be an

alternative method to validate their efficacy.

Another strategy to overcome *EGFR* amplification-mediated resistance is an addition of cetuximab, a human–mouse chimeric antibody that binds to the extracellular domain of EGFR, to third-generation EGFR-TKIs. In previous studies, the efficacy of cetuximab combined with afatinib, a second-generation EGFR-TKI, has been reported^{49, 50,51}. By inhibiting EGF-induced activation of wild-type EGFR in PC9-COR cell line³¹ or dimerization of mutated EGFR induced by EGFR-TKI in erlotinib-resistant *EGFR*-mutated cell lines⁵², cetuximab can enhance the inhibition of third-generation EGFR-TKIs. However, the addition of cetuximab to afatinib did not improve the outcomes in previously untreated *EGFR*-mutant NSCLC patients but led to greater toxicity, including a 72% incidence rate of grade ≥ 3 treatment-related adverse events⁵³.

In summary, this study demonstrated that mutated *EGFR* amplification led to resistance to a third-generation EGFR-TKI, TAS-121, in a patient with *EGFR* T790M-positive NSCLC. Targeting the HSP90 chaperone using TAS-116 overcame this resistance *in vitro* and *in vivo*, indicating a preclinical rationale for the use of HSP90 inhibitors in patients with *EGFR* amplification-mediated resistance to third-generation EGFR-TKIs. Additional investigations into *EGFR* amplification-mediated resistance and the efficacy and safety of HSP90 inhibition are warranted for the development of optimal

therapies.

Acknowledgments

This study was supported by Grants-in-Aid for Scientific Research (Young Scientists no. 17J09900 [Y.T.], and JSPS Research Fellow no. 17K18388 [Y.T.]) from the Ministry of Education, Culture, Sports, Science and Technology of Japan; the Naito Foundation (Y.T.); the Takeda Science Foundation (Y.T.); the Kobayashi Foundation for Cancer Research (Y.T.); the Novartis Foundation Grant (Y.T.); the Bristol-Myers Squibb Foundation Grant (Y.T.); the SGH Foundation (Y.T.); and the National Cancer Center Research and Development Fund (30-A-6 [T.K.]).

Y.G., S.S.K. and Y.T. designed the research; S.W., T.K., and N.M. performed the experiments; S.W., Y.G., and Y.O. obtained the clinical samples and data; S.W., H. Y., H.N., S.S.K., K. K., and Y.T. analyzed the data; and S.W., Y.G., and Y.T. wrote the manuscript. We thank Ms. Tomoka Takaku, Kumiko Yoshida, Konomi Onagawa, Miyuki Nakai, Megumi Takemura, Chie Haijima, Megumi Hoshino, Yoko Shimada and Mr. Hiroki Kakishima for their technical assistance.

Disclosure:

Y.G. received research grant related to this work and honoraria outside this work from Taiho Pharmaceutical. H.N. and S.S.K. received research grant from Taiho Pharmaceutical outside this work. Y.T. received research grants and honoraria from Ono

Pharmaceutical and Bristol-Myers Squibb, research grants from Daiichi-Sankyo and KOTAI Biotechnologies Inc, and honoraria from, AstraZeneca, Chugai Pharmaceutical, and MSD outside this work. All other authors have no competing financial interests.

References

1. Rosell R, Moran T, Queralt C, et al. Screening for epidermal growth factor receptor mutations in lung cancer. *N Engl J Med* 2009; **361**: 958-67.
2. Shi Y, Au JS-K, Thongprasert S, et al. A prospective, molecular epidemiology study of EGFR mutations in Asian patients with advanced non-small-cell lung cancer of adenocarcinoma histology (PIONEER). *J Thorac Oncol* 2014; **9**: 154-62.
3. Ferguson KM. Structure-based view of epidermal growth factor receptor regulation. *Annu Rev Biophys* 2008; **37**: 353-73.
4. Yarden Y, Pines G. The ERBB network: at last, cancer therapy meets systems biology. *Nat Rev Cancer* 2012; **12**: 553-63.
5. Recondo G, Facchinetti F, Olaussen KA, Besse B, Friboulet L. Making the first move in EGFR-driven or ALK-driven NSCLC: first-generation or next-generation TKI? *Nat Rev Clin Oncol* 2018; **15**: 694-708.
6. Mok TS, Wu YL, Thongprasert S, et al. Gefitinib or carboplatin-paclitaxel in pulmonary adenocarcinoma. *N Engl J Med* 2009; **361**: 947-57.
7. Mitsudomi T, Morita S, Yatabe Y, et al. Gefitinib versus cisplatin plus docetaxel in patients with non-small-cell lung cancer harbouring mutations of the epidermal growth factor receptor (WJTOG3405): an open label, randomised phase 3 trial.

Lancet Oncol 2010; **11**: 121-8.

8. Maemondo M, Inoue A, Kobayashi K, et al. Gefitinib or chemotherapy for non-small-cell lung cancer with mutated EGFR. *N Engl J Med* 2010; **362**: 2380-8.
9. Zhou C, Wu YL, Chen G, et al. Erlotinib versus chemotherapy as first-line treatment for patients with advanced EGFR mutation-positive non-small-cell lung cancer (OPTIMAL, CTONG-0802): a multicentre, open-label, randomised, phase 3 study. *Lancet Oncol* 2011; **12**: 735-42.
10. Rosell R, Carcereny E, Gervais R, et al. Erlotinib versus standard chemotherapy as first-line treatment for European patients with advanced EGFR mutation-positive non-small-cell lung cancer (EURTAC): a multicentre, open-label, randomised phase 3 trial. *Lancet Oncol* 2012; **13**: 239-46.
11. Yang JC, Wu YL, Schuler M, et al. Afatinib versus cisplatin-based chemotherapy for EGFR mutation-positive lung adenocarcinoma (LUX-Lung 3 and LUX-Lung 6): analysis of overall survival data from two randomised, phase 3 trials. *Lancet Oncol* 2015; **16**: 141-51.
12. Kobayashi S, Boggon TJ, Dayaram T, et al. EGFR mutation and resistance of non-small-cell lung cancer to gefitinib. *New Engl J Med* 2005; **352**: 786-92.
13. Pao W, Miller VA, Politi KA, et al. Acquired resistance of lung adenocarcinomas to

gefitinib or erlotinib is associated with a second mutation in the EGFR kinase domain.

PLOS Medicine 2005; **2**: e73.

14. Cross DA, Ashton SE, Ghiorghiu S, et al. AZD9291, an irreversible EGFR TKI, overcomes T790M-mediated resistance to EGFR inhibitors in lung cancer. *Cancer Discov* 2014; **4**: 1046-61.
15. Walter AO, Sjin RT, Haringsma HJ, et al. Discovery of a mutant-selective covalent inhibitor of EGFR that overcomes T790M-mediated resistance in NSCLC. *Cancer Discov* 2013; **3**: 1404-15.
16. Ito K, Nishio M, Kato M, et al. TAS-121, a selective mutant EGFR inhibitor, shows activity against tumors expressing various EGFR mutations including T790M and uncommon mutations G719X. *Mol Cancer Ther* 2019; **18**: 920-8.
17. Ramalingam SS, Vansteenkiste J, Planchard D, et al. Overall survival with osimertinib in untreated, EGFR-mutated advanced NSCLC. *New Engl J Med* 2020; **382**: 41-50.
18. Sequist LV, Soria JC, Goldman JW, et al. Rociletinib in EGFR-mutated non-small-cell lung cancer. *New Engl J Med* 2015; **372**: 1700-9.
19. National Comprehensive Cancer Network. NCCN clinical practice guidelines in oncology. Non-small cell lung cancer. Version 5.2020.

20. Ricordel C, Friboulet L, Facchinetti F, Soria JC. Molecular mechanisms of acquired resistance to third-generation EGFR-TKIs in EGFR T790M-mutant lung cancer. *Ann Oncol* 2018; **29**: i28-i37.
21. Leonetti A, Sharma S, Minari R, Perego P, Giovannetti E, Tiseo M. Resistance mechanisms to osimertinib in EGFR-mutated non-small cell lung cancer. *British journal of cancer* 2019; **121**: 725-37.
22. Macario AJ, Conway de Macario E. Sick chaperones, cellular stress, and disease. *New Engl J Med* 2005; **353**: 1489-501.
23. Schopf FH, Biebl MM, Buchner J. The HSP90 chaperone machinery. *Nat Rev Mol Cell Biol* 2017; **18**: 345-60.
24. Hendriks LEL, Dingemans AC. Heat shock protein antagonists in early stage clinical trials for NSCLC. *Expert Opin Investig Drugs* 2017; **26**: 541-50.
25. Felip E, Barlesi F, Besse B, et al. Phase 2 study of the HSP-90 inhibitor AUY922 in previously treated and molecularly defined patients with advanced non-small cell lung cancer. *J Thorac Oncol* 2018; **13**: 576-84.
26. Piotrowska Z, Costa DB, Oxnard GR, et al. Activity of the Hsp90 inhibitor luminespib among non-small-cell lung cancers harboring EGFR exon 20 insertions. *Ann Oncol* 2018; **29**: 2092-7.

27. Ohkubo S, Kodama Y, Muraoka H, et al. TAS-116, a highly selective inhibitor of heat shock protein 90 alpha and beta, demonstrates potent antitumor activity and minimal ocular toxicity in preclinical models. *Mol Cancer Ther* 2015; **14**: 14-22.
28. Sunami K, Ichikawa H, Kubo T, et al. Feasibility and utility of a panel testing for 114 cancer-associated genes in a clinical setting: A hospital-based study. *Cancer Sci* 2019; **110**: 1480-90.
29. Tanabe Y, Ichikawa H, Kohno T, et al. Comprehensive screening of target molecules by next-generation sequencing in patients with malignant solid tumors: guiding entry into phase I clinical trials. *Mol Cancer* 2016; **15**: 73.
30. Varella-Garcia M, Diebold J, Eberhard DA, et al. EGFR fluorescence in situ hybridization assay: guidelines for application to non-small-cell lung cancer. *J Clin Pathol* 2009; **62**: 970-77.
31. Nukaga S, Yasuda H, Tsuchihara K, et al. Amplification of EGFR wild-type alleles in non-small cell lung cancer cells confers acquired resistance to mutation-selective EGFR tyrosine kinase inhibitors. *Cancer Res* 2017; **77**: 2078-89.
32. Nishio M, Murakami H, Ohe Y, et al. Phase I study of TAS-121, a third-generation epidermal growth factor receptor (EGFR) tyrosine kinase inhibitor, in patients with non-small-cell lung cancer harboring EGFR mutations. *Invest New Drugs* 2019; **37**:

- 1207-17.
33. Shimomura A, Yamamoto N, Kondo S, et al. First-in-human phase I study of an oral HSP90 inhibitor, TAS-116, in patients with advanced solid tumors. *Mol Cancer Ther* 2019; **18**: 531-40.
 34. Doi T, Kurokawa Y, Sawaki A, et al. Efficacy and safety of TAS-116, an oral inhibitor of heat shock protein 90, in patients with metastatic or unresectable gastrointestinal stromal tumour refractory to imatinib, sunitinib and regorafenib: a phase II, single-arm trial. *Eur J Cancer* 2019; **121**: 29-39.
 35. Piotrowska Z, Niederst MJ, Karlovich CA, et al. Heterogeneity underlies the emergence of EGFR T790 wild-type clones following treatment of T790M-positive cancers with a third-generation EGFR inhibitor. *Cancer Discov* 2015; **5**: 713-22.
 36. Ramalingam SS, Yang JCH, Lee CK, et al. Osimertinib as first-line treatment of EGFR mutation–positive advanced non–small-cell lung cancer. *J Clin Oncol* 2017; **36**: 841-9.
 37. Schoenfeld AJ, Yu HA. The evolving landscape of resistance to osimertinib. *J Thorac Oncol* 2020; **15**: 18-21.
 38. Chabon JJ, Simmons AD, Lovejoy AF, et al. Circulating tumour DNA profiling reveals heterogeneity of EGFR inhibitor resistance mechanisms in lung cancer

- patients. *Nat Commun* 2016; **7**: 11815.
39. Nakatani K, Yamaoka T, Ohba M, et al. KRAS and EGFR amplifications mediate resistance to rociletinib and osimertinib in acquired afatinib-resistant NSCLC harboring exon 19 deletion/T790M in EGFR. *Mol Cancer Ther* 2019; **18**: 112-26.
40. Kim TM, Song A, Kim DW, et al. Mechanisms of acquired resistance to AZD9291: A mutation-selective, irreversible EGFR inhibitor. *J Thorac Oncol* 2015; **10**: 1736-44.
41. Knebel FH, Bettoni F, Shimada AK, et al. Sequential liquid biopsies reveal dynamic alterations of EGFR driver mutations and indicate EGFR amplification as a new mechanism of resistance to osimertinib in NSCLC. *Lung Cancer* 2017; **108**: 238-41.
42. Roper N, Brown A-L, Wei JS, et al. Clonal evolution and heterogeneity of osimertinib acquired resistance mechanisms in EGFR mutant lung cancer. *Cell Reports Medicine* 2020; **1**: 100007.
43. Garcia-Carbonero R, Carnero A, Paz-Ares L. Inhibition of HSP90 molecular chaperones: moving into the clinic. *Lancet Oncol* 2013; **14**: e358-e69.
44. Shimamura T, Li D, Ji H, et al. Hsp90 inhibition suppresses mutant EGFR-T790M signaling and overcomes kinase inhibitor resistance. *Cancer Res* 2008; **68**: 5827-38.
45. Wang S, Pashtan I, Tsutsumi S et al. Cancer cells harboring MET gene amplification

- activate alternative signaling pathways to escape MET inhibition but remain sensitive to Hsp90 inhibitors. *Cell Cycle* 2009; **8**: 2050-56.
46. Koizumi H, Yamada T, Takeuchi S, et al. Hsp90 inhibition overcomes HGF-triggering resistance to EGFR-TKIs in EGFR-mutant lung cancer by decreasing client protein expression and angiogenesis. *J Thorac Oncol* 2012; **7**: 1078-85.
47. Codony-Servat J, Viteri S, Codony-Servat C, et al. Hsp90 inhibitors enhance the antitumoral effect of osimertinib in parental and osimertinib-resistant non-small cell lung cancer cell lines. *Transl Lung Cancer Res* 2019; **8**: 340-51.
48. Aguila M, Bevilacqua D, McCulley C, et al. Hsp90 inhibition protects against inherited retinal degeneration. *Hum Mol Genet* 2014; **23**: 2164-75.
49. Regales L, Gong Y, Shen R, et al. Dual targeting of EGFR can overcome a major drug resistance mutation in mouse models of EGFR mutant lung cancer. *J Clin Invest* 2009; **119**: 3000-10.
50. Janjigian YY, Smit EF, Groen HJ, et al. Dual inhibition of EGFR with afatinib and cetuximab in kinase inhibitor-resistant EGFR-mutant lung cancer with and without T790M mutations. *Cancer Discov* 2014; **4**: 1036-45.
51. Pirazzoli V, Ayeni D, Meador CB et al. Afatinib plus cetuximab delays resistance compared to single-agent erlotinib or afatinib in mouse models of TKI-naive EGFR

L858R-induced lung adenocarcinoma. *Clin Cancer Res* 2016; **22**: 426-35.

52. Oashi A, Yasuda H, Kobayashi K et al. Monomer preference of EGFR tyrosine kinase inhibitors influences the synergistic efficacy of combination therapy with cetuximab.

Mol Cancer Ther 2019; **18**: 1593-1601.

53. Goldberg SB, Redman MW, Lilenbaum R et al. Randomized trial of afatinib plus cetuximab versus afatinib alone for first-line treatment of EGFR-mutant non-small-cell lung cancer: final results from SWOG S1403. *J Clin Oncol* 2020; **38**: 4076-85.

Figure Legends

Figure 1. Clinical course.

A 68-year-old woman with metastatic lung adenocarcinoma (cT4N2M1b) harboring an *EGFR* L858R mutation received gefitinib and achieved a PR. Eleven months later, she experienced PD and received chemotherapy. Liver biopsy of progressing liver metastases indicated a secondary mutation of *EGFR* T790M in addition to the primary mutation. She was treated with TAS-121 in a phase I trial. Despite the initial response, PD was confirmed by CT showing regrowth of liver lesions. She died 4 months after initiation of TAS-121 treatment.

Figure 2. EGFR gene status.

A, NGS of the *EGFR* gene. The post-TAS-121-treatment liver sample was analyzed using NGS. The *EGFR* mutation (left) and copy number gain (right, red) are shown. Blue, wild-type allele; red, T790M-mutated allele. **B**, FISH. We conducted FISH analyses of *EGFR* using FFPE samples from the pre-TAS-121-treatment liver lesion, the post-TAS-121-treatment liver lesion, and autopsied lung and liver lesions. Green, *CEP*; red, *EGFR*.

Figure 3. Sensitivities of *EGFR*-mutated cell lines to EGFR-TKIs.

A, Cell proliferation assay of several *EGFR*-mutated cell lines under EGFR-TKIs. HCC827 (left), PC-9 (middle), and H1975 (right) cells were plated in 96-well plates at a density of 2×10^3 cells/well, and cell proliferation was evaluated with the WST-1 assay following 72 hours of treatment. Experiments were independently performed in triplicate, and the means are shown. Black, erlotinib; red, osimertinib; blue, TAS-121. **B and C**, Western blotting in PC-9 (B) and H1975 cell lines (C). Cells were cultured with the indicated concentrations of EGFR-TKIs for 3 hours, and then the cell lysates were subjected to western blot analysis. GAPDH was used as the internal control. Representative data from three independent experiments are shown. **D and E**, Apoptosis in the PC-9 (D) and H1975 (E) cell lines. Apoptosis was assessed using flowcytometry with FITC-annexin V and 7-AAD after 72 hours of treatment. Representative data from three independent experiments (left), and the mean and SEM values (right) are shown. *, $p < 0.05$; NS, not significant.

Figure 4. Sensitivities of the H1975-LR/TM cell line to EGFR-TKIs or TAS-116.

A, Western blotting in H1975 cell lines. H1975 cells with overexpression of *EGFR* L858R/T790M (H1975-LR/TM) were generated by retroviral transduction, and EGFR expression was analyzed by western blotting. GAPDH was used as the internal control.

Representative data from three independent experiments are shown. **B**, Cell proliferation assay of the H1975-LR/TM cell line under EGFR-TKIs or TAS-116. Cells were plated in 96-well plates at a density of 2×10^3 cells/well, and cell proliferation was evaluated with a WST-1 assay after 72 hours of treatment. Experiments were independently performed in triplicate, and the means are shown. Red, osimertinib; blue, TAS-121; green, TAS-116.

C, Western blot analysis of the H1975-LR/TM cell line. Cells were cultured with the indicated concentrations of EGFR-TKIs for 3 hours or TAS-116 for 48 hours, and the cell lysates were then subjected to western blot analysis. GAPDH was used as the internal control. Representative data from three independent experiments are shown. **D**, Apoptosis in the H1975 cell-LR/TM cell line. Apoptosis was assessed using flowcytometry with FITC-annexin V and 7-AAD after 72 hours of treatment. Representative data from three independent experiments (left), and the mean and SEM values (right) are shown. *, $p < 0.05$; NS, not significant.

Figure 5. Sensitivities of the PC9-COR cell line to EGFR-TKIs and TAS-116.

A, Western blot analysis of the cell lines. EGFR with exon 19 deletion was detected using a specific antibody. GAPDH was used as the internal control. Representative data from three independent experiments are shown. **B**, Cell proliferation assay of the PC9-COR

cell line under treatment with EGFR-TKIs or TAS-116. Cells were plated in 96-well plates at a density of 2×10^3 cells/well, and cell proliferation was evaluated with a WST-1 assay after 72 hours of treatment. Experiments were performed independently in triplicate, and the means are shown. Black, erlotinib; red, osimertinib; blue, TAS-121; green, TAS-116. **C**, Western blot analysis of the PC9-COR cell line. Cells were cultured with the indicated concentrations of EGFR-TKIs for 3 hours or with TAS-116 for 48 hours, and the cell lysates were then subjected to western blot analysis. GAPDH was used as the internal control. Representative data from three independent experiments are shown. **D**, Apoptosis in the PC9-COR cell line. Apoptosis was assessed using flowcytometry with FITC-annexin V and 7-AAD after 72 hours of treatment. Representative data from three independent experiments (top), and the mean and SEM values (bottom) are shown. *, $p < 0.05$; NS, not significant.

Figure 6. *In vivo* effects of TAS-116 against H1975-LR/TM and PC9-COR tumors.

A, *In vivo* efficacy of TAS-121 against H1975 tumors. Cells (1×10^6) in 100 μ L of RPMI with 100 μ L of Matrigel were injected subcutaneously, and the tumor volume was assessed twice a week using the formula “length \times width² \times 0.5.” The mice were grouped when the tumor volume reached approximately 200–500 mm³. TAS-121 (12.5

mg/kg/day) and the vehicle were orally administered daily thereafter. **B and C**, *In vivo* efficacy of TAS-116 against H1975-LR/TM (B) and PC9-COR (C) tumors. *In vivo* experiments were performed as described in A. TAS-116 (14 mg/kg/day) was administered orally five times a week. The mean and SEM values are shown. *, $p < 0.05$; NS, not significant.

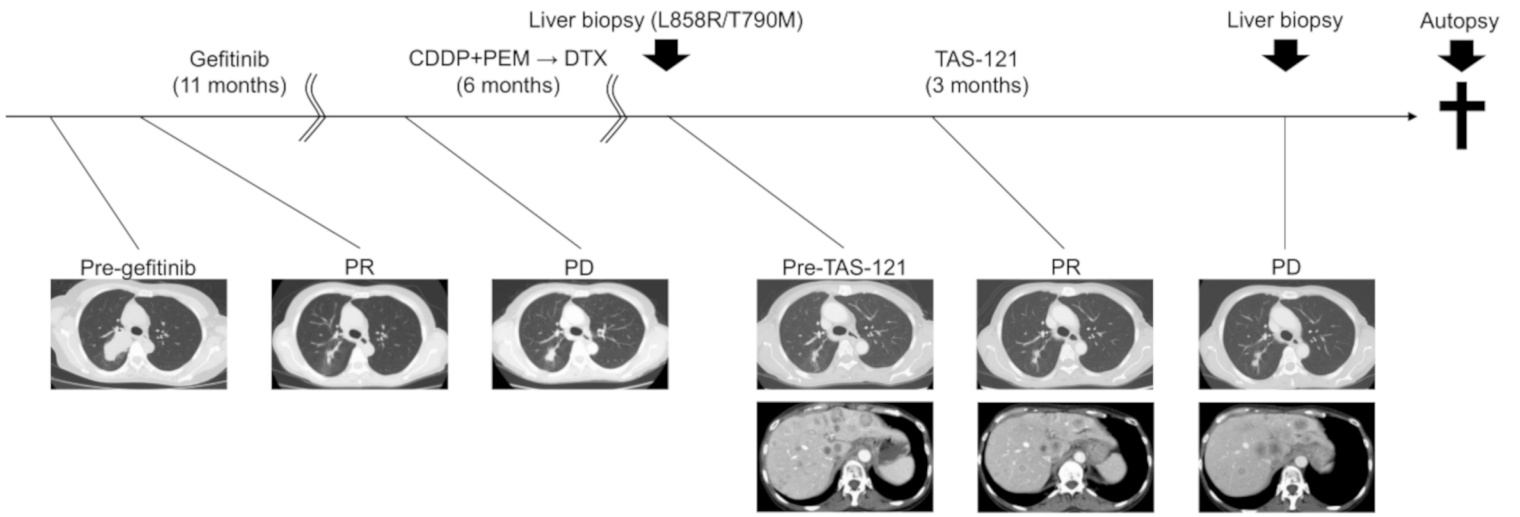


Figure 1

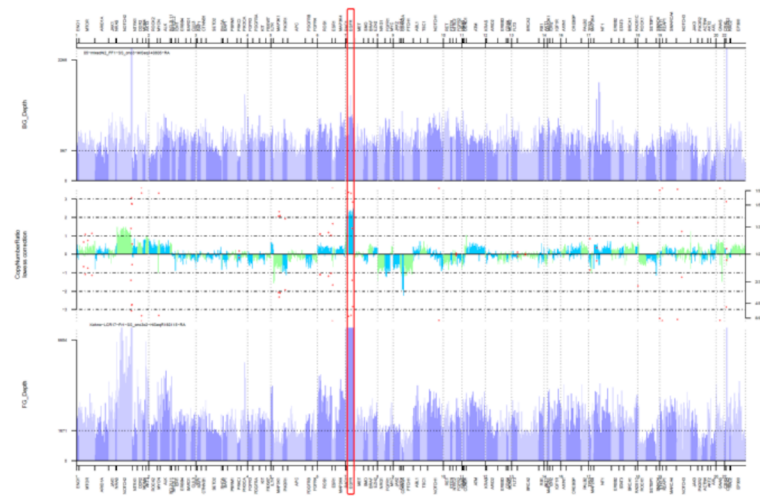
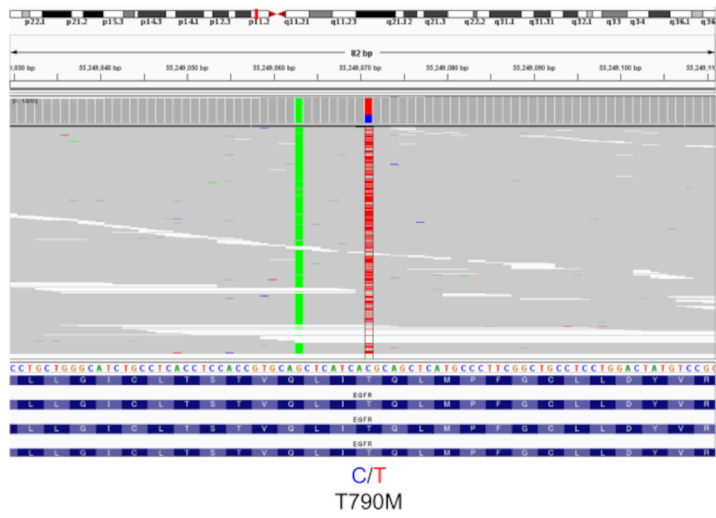
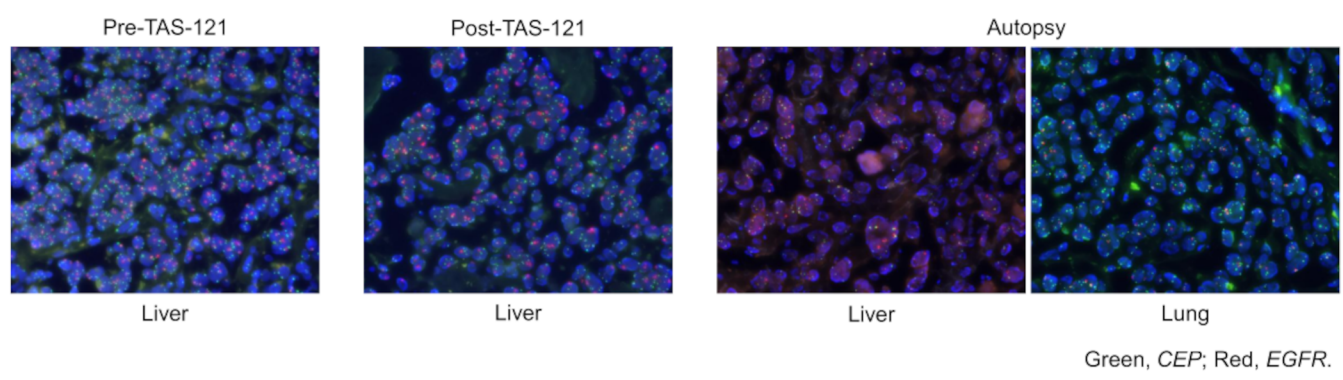
A**B**

Figure 2

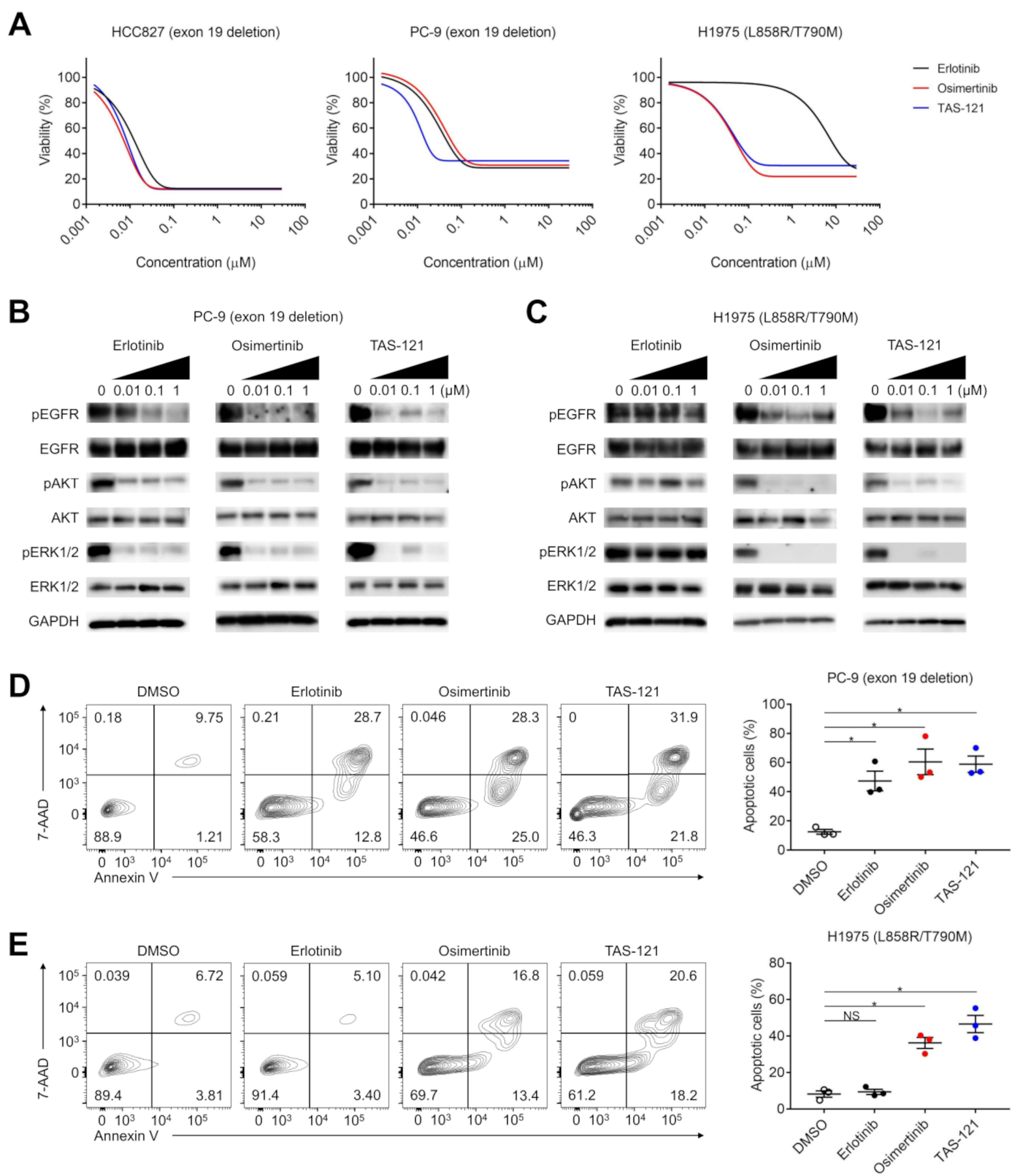


Figure 3

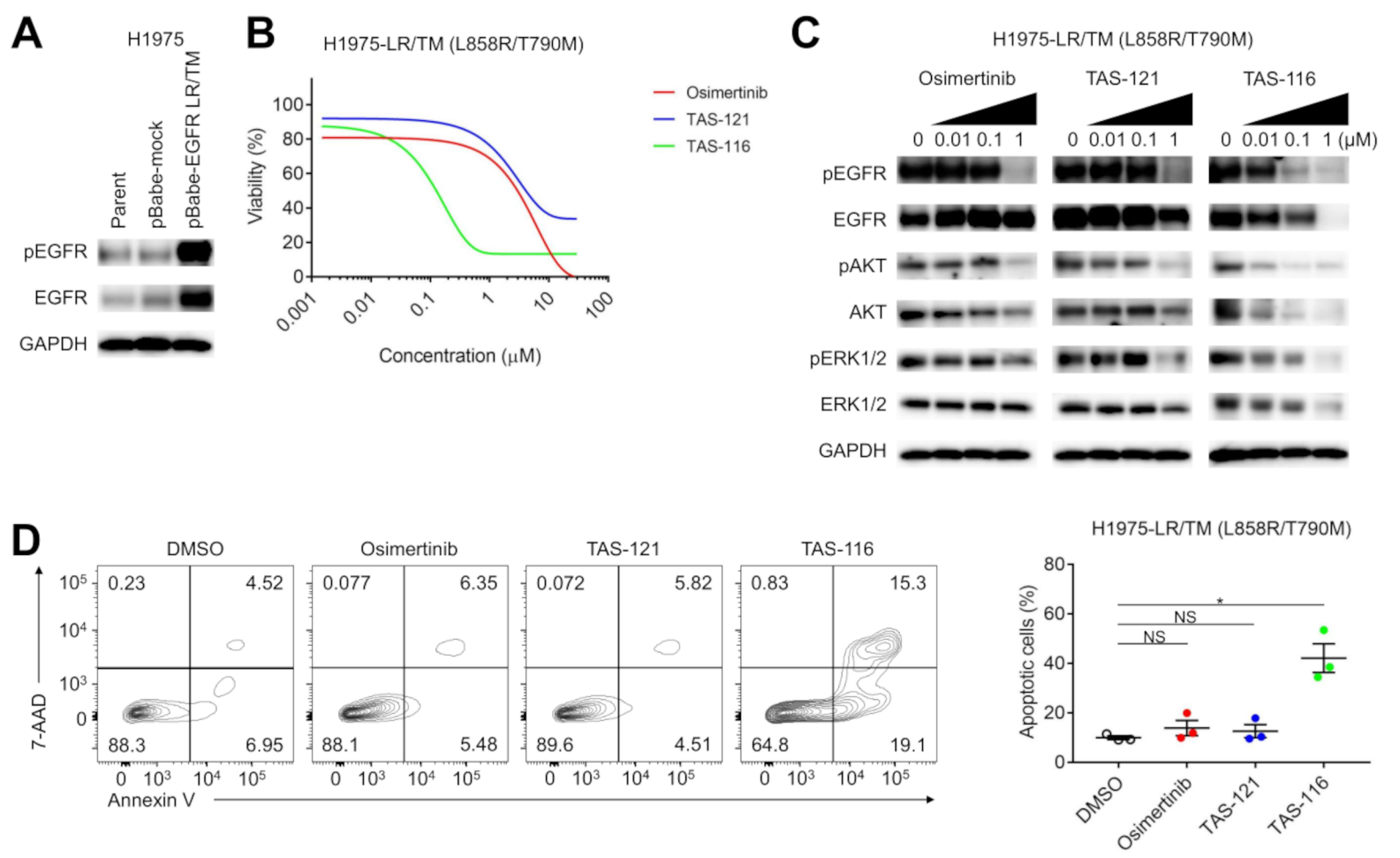


Figure 4

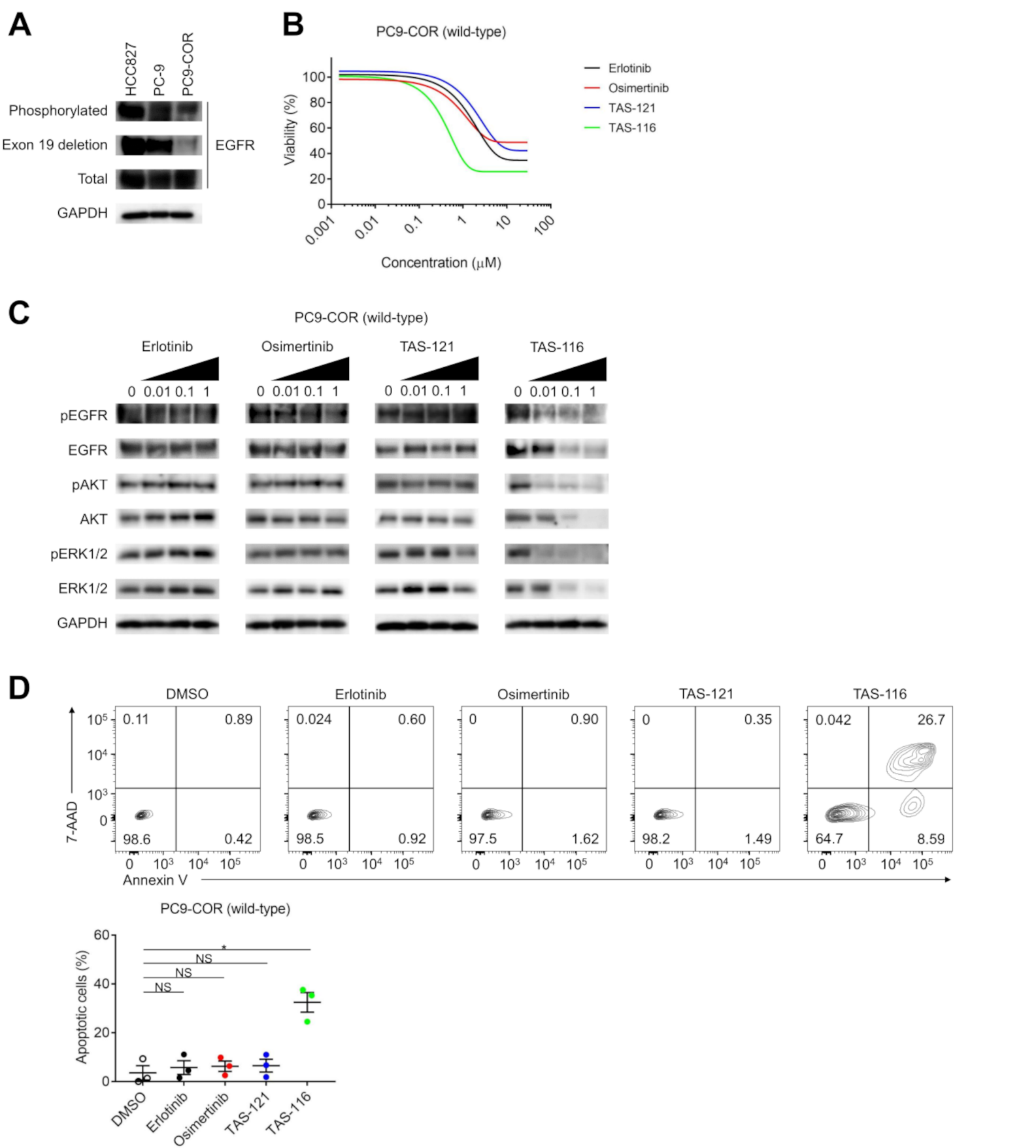


Figure 5

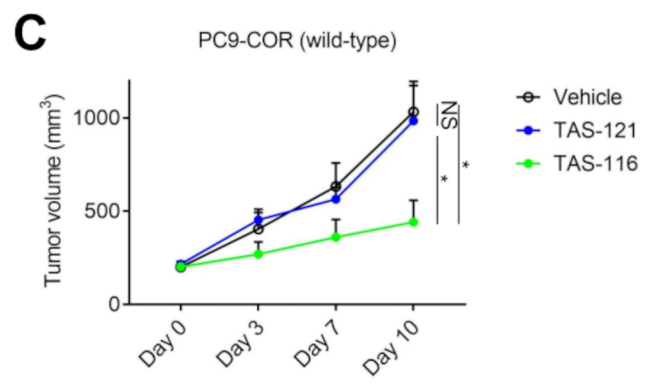
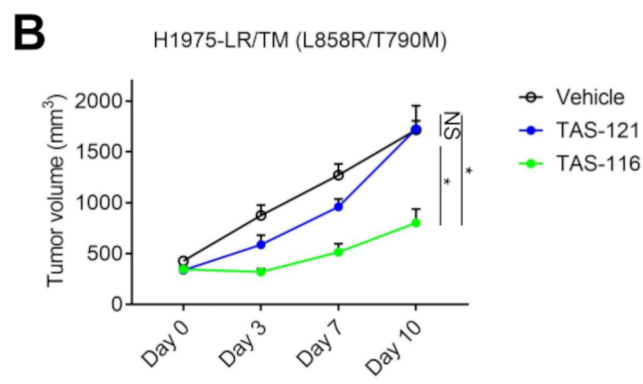
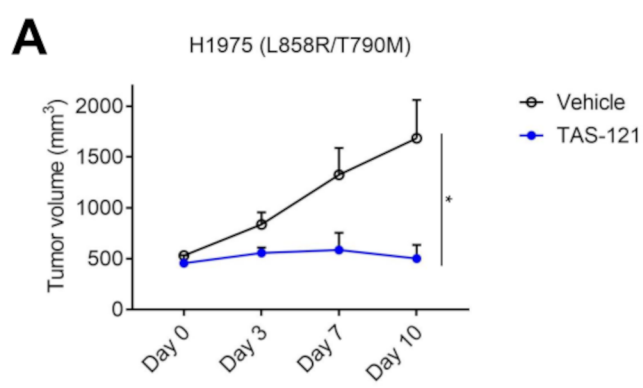
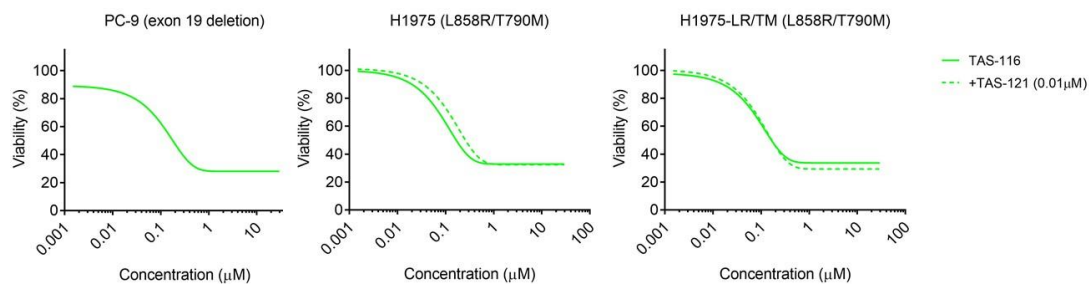


Figure 6

Supplementary Figure S1. Sensitivities of *EGFR*-mutated NSCLC cell lines to TAS-116 with or without TAS-121 (0.01 μ M).



Cells were plated in 96-well plates at a density of 2×10^3 cells/well, and cell proliferation was evaluated with a WST-1 assay after 72 hours of treatment. Experiments were performed independently in triplicate.

Supplementary Table S1. Lists of 104 genes examined by NCC Oncopanel v3 test.

Mutation and copy number alterations for all exons				Fusion	
<i>ABL1</i>	<i>CREBBP</i>	<i>IL7R</i>	<i>NTRK1</i>	<i>SMAD4</i>	<i>ALK</i>
<i>ACTN4</i>	<i>CTNNB1</i>	<i>JAK1</i>	<i>NT5C2</i>	<i>SMARCA4</i>	<i>AKT3</i>
<i>AKT1</i>	<i>CUL3</i>	<i>JAK2</i>	<i>PALB2</i>	<i>SMO</i>	<i>AXL</i>
<i>AKT2</i>	<i>DDR2</i>	<i>JAK3</i>	<i>PBRM1</i>	<i>STAT3</i>	<i>BRAF</i>
<i>AKT3</i>	<i>EGFR</i>	<i>KEAP1</i>	<i>PDGFRA</i>	<i>STK11</i>	<i>EGFR</i>
<i>ALK</i>	<i>ENO1</i>	<i>KIT</i>	<i>PDGFRB</i>	<i>TP53</i>	<i>ERBB4</i>
<i>APC</i>	<i>EP300</i>	<i>KRAS</i>	<i>PIK3CA</i>	<i>TSC1</i>	<i>FGFR1</i>
<i>ARID1A</i>	<i>ERBB2</i>	<i>MAP2K1</i>	<i>PIK3R1</i>	<i>VHL</i>	<i>FGFR2</i>
<i>ARID2</i>	<i>ERBB3</i>	<i>MAP2K4</i>	<i>PIK3R2</i>		<i>FGFR3</i>
<i>ATM</i>	<i>ERBB4</i>	<i>MAP3K1</i>	<i>PRKCI</i>		<i>NOTCH1</i>
<i>AXIN1</i>	<i>ESR1</i>	<i>MAP3K4</i>	<i>PTCH1</i>		<i>NRG1</i>
<i>AXL</i>	<i>EZH2</i>	<i>MDM2</i>	<i>PTEN</i>		<i>NTRK1</i>
<i>BAP1</i>	<i>FBXW7</i>	<i>MDM4</i>	<i>RAC1</i>		<i>PDGFRA</i>
<i>BARD1</i>	<i>FGFR1</i>	<i>MET</i>	<i>RAC2</i>		<i>RAF1</i>
<i>BCL2L11</i>	<i>FGFR2</i>	<i>MTOR</i>	<i>RAD51C</i>		<i>RET</i>
<i>BRAF</i>	<i>FGFR3</i>	<i>MYC</i>	<i>RAF1</i>		<i>ROS1</i>
<i>BRCA1</i>	<i>FGFR4</i>	<i>MYCN</i>	<i>RB1</i>		
<i>BRCA2</i>	<i>FLT3</i>	<i>NF1</i>	<i>RET</i>		
<i>CCND1</i>	<i>GNAS</i>	<i>NFE2L2</i>	<i>RHOA</i>		
<i>CD274</i>	<i>HRAS</i>	<i>NOTCH1</i>	<i>ROCK1</i>		
<i>CDK4</i>	<i>IDH1</i>	<i>NOTCH2</i>	<i>ROCK2</i>		
<i>CDKN2A</i>	<i>IDH2</i>	<i>NOTCH3</i>	<i>ROS1</i>		
<i>CHEK2</i>	<i>IGF1R</i>	<i>NRAS</i>	<i>SETBP1</i>		
<i>CRKL</i>	<i>IGF2</i>	<i>NRG1</i>	<i>SETD2</i>		

Supplementary Table S2. *EGFR* mutational statuses of cell lines.

Cell line	Genetic alterations
HCC827	<i>EGFR</i> E746_A750del
PC-9	<i>EGFR</i> E746_A750del
PC9-COR	Wild-type <i>EGFR</i> amplification
H1975	<i>EGFR</i> L858R/T790M
H1975-LR/TM	<i>EGFR</i> L858R/T790M + <i>EGFR</i> L858R/T790M overexpression

Supplementary Table S3. Summary of antibodies for western blotting.

Molecule	Clone	Host	Company
Human EGFR	D38B1	Rabbit	Cell Signaling Technology
Human pEGFR	D7A5	Rabbit	Cell Signaling Technology
Human ex 19 deleted EGFR	D6B6	Rabbit	Cell Signaling Technology
Human AKT	Polyclonal	Rabbit	Cell Signaling Technology
Human pAKT (Ser473)	D9E	Rabbit	Cell Signaling Technology
Human ERK1/2	137F5	Rabbit	Cell Signaling Technology
Human pERK1/2	D13.14.4E	Rabbit	Cell Signaling Technology
Human GAPDH	D16H11	Rabbit	Cell Signaling Technology

Supplementary Table S4. Summary of genetic alterations.

Mutation	Fusion	Copy number variation
<i>EGFR</i> L858R	Not detected	<i>NOTCH2</i> amplification
<i>EGFR</i> T790M		<i>RAC1</i> amplification
<i>TP53</i> L194fs		<i>EGFR</i> amplification
		<i>CDKN2A</i> homozygous deletion